Blood First Edition Paper, prepublished online January 18, 2008; DOI 10.1182/blood-2007-07-103309

VAMP-8 segregates mast cell preformed mediator exocytosis from cytokine trafficking pathways

Neeraj Tiwari[12], Cheng-Chun Wang[3], Cristiana Brochetta[12], Gou Ke[3], Francesca Vita[4], Zeng Qi[3], Juan Rivera[5], Maria Rosa Soranzo[4], Giuliano Zabucchi[4], Wanjin Hong[3] and Ulrich Blank*[12]

[1]Inserm U699, Paris, F-75018, France

[2]Université Paris 7-Denis Diderot, Faculté de Médecine, Site Xavier Bichat, Paris, F-75018, France

[3]Membrane Biology Laboratory, Institute of Molecular and Cellular Biology, Proteos, Singapore 138673, Singapore

[4]Department of Physiology and Pathology, University of Trieste, Italy

[5]Laboratory of Immune Cell Signaling, National Institute of Arthritis and Musculoskeletal and Skin Diseases, National Institutes of Health, Building 10, Room 9N228, Bethesda, MD 20892-1820, USA

Running title: Role of VAMP-8 in mast cell exocytosis

Keywords: SNARE, VAMP-8, exocytosis, mast cells

* Address correspondence to Dr Ulrich Blank, Inserm U699, Immunopathologie rénale, récepteurs et inflammation, Faculté de Medicine Paris 7, Site Xavier Bichat, 16- rue Henri Huchard, BP416 75870 Paris France email: ublank@bichat.inserm.fr

Abstract

Inflammatory responses by mast cells are characterized by massive exocytosis of prestored granular mediators followed by cytokine/chemokine release. The vesicular trafficking mechanisms involved remain poorly understood. Vesicular Associated Membrane Protein-8 (VAMP-8), a member of the v-SNARE family of fusion proteins initially characterized in endosomal and endosomal-lysosomal fusion may also function in regulated exocytosis. Here we show that in bone marrow derived mast cells (BMMCs) VAMP-8 partially colocalized with secretory granules and redistributed upon stimulation. This was associated with increased SNARE complex formation with the target t-SNAREs, SNAP-23 and syntaxin-4. VAMP-8-deficient BMMCs exhibited a markedly reduced degranulation response after IgE+antigen-, thapsigargin- or ionomycin-induced stimulation. VAMP-8-deficient mice also showed reduced plasma histamine levels in passive systemic anaphylaxis experiments, while cytokine/chemokine release was not affected. Unprocessed TNF accumulated at the plasma membrane where it colocalized with a VAMP-3-positive vesicular compartment but not with VAMP-8. The findings demonstrate that VAMP-8 segregates secretory lysosomal granules exocytosis in mast cells from cytokine/chemokine molecular trafficking pathways.

Introduction

Mast cells are granulated cells of hematopoetic origin localized to tissues that play a role in innate and adaptive defense to pathogens as well as in various inflammatory and immunoregulatory responses. They are also central effectors in anaphylaxis, allergy and asthma [1-3]. These functions depend on the release of pro-inflammatory mediators following activation through cell surface receptors such as the high affinity IgE receptor (FcεRI) [4]. The mast cell inflammatory response is characterized by an early phase with massive discharge of mediators stored in cytoplasmic secretory granules (SGs) through multigranular/compound exocytosis and a late phase that involves generation of arachidonic acid metabolites and *de novo* synthesis of cytokines/chemokines and growth factors released through vesicular carriers [2-4].

The signaling events required for degranulation and cytokine/chemokine secretion, although involving common initial elements, are distinct and depend on particular regulatory requirements of each pathway. In agreement, deficiency in Bcl10 or Malt1, a signaling complex upstream of NF-κB, affected cytokine production but not mast cell degranulation [5]. Both processes are also likely regulated at the level of intracellular trafficking and fusion. Cytokine release is still poorly characterized, but involves vesicular carriers along the secretory pathway. In macrophages it has been shown that these vesicles fuse with recycling endosomes to discharge at specific sites at the phagocytic cup [6,7].

Mast cell SGs are secretory lysosomes with an intimate connection between the secretory and endocytic pathway, as in other hematopoietic cells [8-11]. The protein sorting to these compartments is regulated by synaptotagmins [9,12] as well as Munc13-4 and rab27a as shown in cytotoxic T cells [11]. Furthermore, constitution of an appropriate granular compartment and proper loading of prestored inflammatory mediators depend

partly on proteoglycans expression. Genetic targeting of the heparin biosynthesis pathway or the serglycin core in mice revealed severe defects in SG maturation [13-15]. Release from SGs in mast cells involves soluble *N*-ethylmaleimide-sensitive factor (NSF) attachment protein receptors (SNAREs) membrane fusion proteins. These are divided into vesicular or v-SNAREs including VAMP family members and target or t-SNAREs including syntaxins and soluble NSF attachment proteins (SNAP) family members. SNAREs contain an about 60 aa α-helical SNARE motif, four of which combine to form a stable tetrameric core complex that catalyzes membrane fusion [16]. Previous studies demonstrated that mast cells utilize the t-SNAREs SNAP-23 and syntaxin-4 in IgE-dependent degranulation [17-19]. Several VAMP proteins are expressed in mast cells including VAMP-2, VAMP-3, VAMP-7 and VAMP-8 [18,20]. The latter showed significant colocalization with SGs, while for the others co-localisation was minor. However, evidence for the function of v-SNAREs in mast cell degranulation is limited. Similarly, data about involvement of SNARE proteins in cytokine secretion are non-existent, with the exception that prestored TNF may be transported into this compartment after re-endocytosis of newly synthesized protein [21] or involve a N-linked glycosylation dependent sorting mechanism [22]. In macrophages TNF secretion involves a vesicular compartment containing syntaxin-6, syntaxin-7 and Vti1b (Vesicle transport through interaction with t-SNARE homologue 1b) that fuses with VAMP-3-positive recycling endosomes to mediate specific delivery at the phagocytotic cup [6].

The v-SNARE VAMP-8, also known as endobrevin, is expressed in many organs and tissues including lungs, kidney, heart, salivary glands [23] but not in neurons [24]. It was initially characterized as a v-SNARE involved in homotypic fusion of early and late endosomes [24,25] and in the heterotypic fusion between late endosomes and lysosomes [26]. More recently it was demonstrated to play a role in regulated exocytosis in the pancreas and other glands of the exocrine system [23,27] as well as in platelets [28]. Based

on previous data showing that mast cell secretory lysosomes contain VAMP-8 [18], we examined whether this v-SNARE protein plays a role in mast cell degranulation and cytokine secretion by analyzing cells from VAMP-8-deficient mice. Our findings demonstrate that VAMP-8 is part of a trafficking pathway that distinguishes degranulation from cytokine release.

Material and methods

Reagents and antibodies

Rabbit Abs to syntaxin-2, syntaxin-3, syntaxin-4, SNAP-23, VAMP-4, VAMP-8, Munc18-2 have been described [18,29,30]. Mouse monoclonal anti-DNP-IgE [18] was used either as ascites or after affinity purification. Mouse monoclonal VAMP-2 (clone Cl 69.1), rabbit SNAP-23 antibodies and rabbit anti-VAMP-3 (for biochemistry) were from Synaptic Systems (Göttingen, Germany). Rabbit anti-VAMP-3 (for confocal imaging) was from Novus Biologicals (Littelton, CO). Monoclonal mouse anti-serotonin (clone 5HT-H209) was from Dako (Glostrup, Denmark). Rat monoclonal anti-mouse mMCP-6 (tryptase) and rat monoclonal anti-serotonin (cloneYC5/45) were purchased from R&D Systems (Lille, France) and AbDSerotec (Oxford, UK), respectively. Mouse anti-β-actin mAb, p-nitrophenyl N-acetyl-β-D-glucosaminide were from Sigma-Aldrich (Saint-Quentin Fallavier, France). Hamster anti-mouse FcεRI, rat anti mouse c-kit-biotin, SA-PE and rat anti-mouse mAb TNF coupled to Cy5 antibodies were from eBioscience (San Diego, CA). Anti-rabbit alexa 488, anti-mouse alexa 568 and SA-647 were from Molecular Probes (Eugene, OR). Goat anti-rat IgG:Dylight549 (mouse adsorbed) was obtained from AbDSerotec. IL3 and SCF were purchased from Peprotech (Levallois, France). Murine IL-1β was purchased from ProSpec Tany Technogene, Rehovot, Israel). Murine cytokines/chemokine detection Duoset ELISA kits (IL-4, IL-6, TNF and MIP-1α) were

purchased from R&D systems. The TNF converting enzyme (TACE) inhibitor TAPI-1, ionomycin, thapsigargin and PMA were all from Calbiochem (La Jolla, CA).

Mice

The generation of VAMP-8-deficient mice was reported previously [27]. Mice were housed under specific pathogen-free conditions at Biological Resource Center (BRC), Institute of Molecular and Cell Biology, Singapore. Mice were maintained in the 129/SvJ background and genotyping was performed as before. All experiments were done in accordance with national guidelines and approved by an institutional ethics committee.

Histology

Ear, abdominal skin and ear tissues from three sets of WT and VAMP-8-deficient mice were collected and fixed in 10 % formalin. After paraffin embedding, 5 µm sections were cut and stained with toluidine blue. Metachromatically stained mast cells were enumerated by counting 5 high power fields (40 x) per section using a Leica DFC320 microscope. Mast cells were also obtained from peritoneal cavity and were stained using toluidine blue.

Mast cell isolation and culture

Bone marrow cells isolated from the femurs of VAMP-8-deficient mice were washed in complete IMDM medium containing 15% FCS, 25 mM HEPES pH 7.4, 1 mM Sodium pyruvate, 1% non-essential amino acid, 54 µM β-mercaptoethanol with 100 U/ml of penicillin, and 100 µg/ml of streptomycin (Invitrogen), and were then cultured in complete medium containing 10 ng/ml IL-3 and and 10 ng/ml SCF for 4 to 8 weeks to obtain bone marrow derived mast cells (BMMCs). Every five days medium was replaced. All cell cultures were grown at 37°C in a humidified atmosphere with 5% CO_2. Rat peritoneal mast cells (RPMC) were obtained by peritoneal lavage with 50 ml icecold PBS/0.1% BSA using Wistar male or female rats purchased from the animal facility of the University

of Trieste. Rats were killed using CO_2 inhalation. The cell suspension was centrifuged at 200xg for 8 min at 4°C and mast cells were purified over 0.883g/ml (d20°C) one-step Percoll gradient containing 0.1% BSA. Final population of mast cells in pellet was > 98%.

Flow cytometric analysis of c-kit and FcεRI expression

BMMCs were washed with ice-cold PBS and indirect immunofluorescence staining was performed with rat anti-mouse c-kit-biotin followed by SA-PE and hamster anti-mouse FcεRI followed by anti-hamster biotin and SA-PE.

Passive systemic anaphylaxis experiments

Mice were sensitized by i.v. injection using 30 µg of purified anti-DNP IgE [18]. After 24 h they were challenged i.v. with 100 µg of DNP-HSA (Sigma) in 200 µl of PBS for 2 min and blood was collected in ice-cold 5 µl heparin-containing tubes. Serum histamine concentration was determined using a histamine immunoassay kit (Beckman coulter, Marseille, France) according to the manufacturer's instructions.

Degranulation measurements

Release of prestored granular mediators was determined by measuring the release of β-hexosaminidase or histamine [18]. Briefly, 4 to 6 week old BMMC (2×10^6/ml) were sensitized overnight with anti-DNP IgE in IL3 and SCF-containing complete medium. To measure release, sensitized cells were washed two times with Tyrode's buffer and stimulated with indicated concentrations of DNP-HSA, ionomycin/PMA or thapsigargin for indicated times. Following stimulations cells were placed on ice for 10 min and centrifuged at 300 x g for 10 min at 4°C. The enzymatic activities of β-hexosaminidase in supernatants and in cells solubilized with 0.5% Triton X-100, were determined as described earlier [18]. Histamine concentration was determined as above.

Determination of cytokine production

BMMCs were sensitized with anti-DNP IgE overnight. After washing BMMCs were resuspended in growth factor containing complete medium at 1 x 10^6 cells/ ml in 24 well tissue culture plates. Cells were stimulated with DNP-HSA (10 ng/ml) over different time points at 37°C. Supernatants were collected and TNF, IL-6, IL-4 or MIP-1α were quantified using Duoset cytokine ELISA kits according to the manufacturer's instructions. MIP-1α secretion was also determined after stimulation with ionomycin (1 μM)/PMA (20 nM) or IL-1β (25 ng/ml).

Immunoblotting and immunoprecipitation

Two million cells (in 1 ml complete growth factor-containing medium) were sensitized overnight with anti-DNP IgE. After washing, cells were resuspended in Tyrode's buffer and challenged with DNP-HSA (10 ng/ml). Stimulation was arrested using ice-cold PBS. Cell lysates were prepared in 50 mM HEPES pH7.2 containing 1% Triton X-100, 0.1 % SDS, 50 mM NaCl, 50 mM NaF, 1 mM sodium orthovanadate and protease inhibitors aprotinin 1000 U/ml (Sigma), pepstatin 10 μg/ml, leupeptin 20 μg/ml and AEBSF 2 μM (Alexis Inc.). For immunoprecipitation, cells were lysed in buffer containing 0.5% Triton X-100 and 0.5 % Octylglucoside for 30 min at 4°C. In some experiments cells were also treated with 1mM N-ethylmaleimide (NEM) before lysis as described [18]. Proteins were resolved on SDS-PAGE and transferred onto nitrocellulose membrane (Schleicher & Schuell, Dassel, Germany) or PVDF (Sigma). Membranes were blocked with 4 % BSA for 1 h followed by incubation with primary antibodies (1 h at RT). After several washes, blots were incubated with donkey anti-rabbit IgG HRP (1/30000) or goat anti-mouse IgG HRP (1/20000) (Jackson Immunoresearch, Nemarket, UK) or Protein A HRP (1/40000) (Sigma) for 45 min and were developed by ECL (GE, Paris, France). Quantification analysis of co-immunoprecipitated complexes was performed using Image J software.

Confocal microscopy

For confocal immunofluorescence microscopy, BMMCs were seeded in 24-well plates on coverslips coated with 0.025% (w/v) poly-L-lysine (Sigma) for 4 hours at 37°C in a humidified atmosphere with 5% CO_2. After stimulation cells were washed twice with ice-cold PBS and fixed for 20 min on ice in 10 mM PIPES pH 6.8, 150 mM NaCl, 5 mM EGTA, 5 mM $MgCl_2$, 5 mM glucose containing 4% paraformaldehyde (IF buffer) followed by 2 washes in IF buffer for 2 min. Fixed cells were permeabilized in IF buffer containing 0.025 % saponin for 20 min at room temperature, followed by blocking in IF buffer containing 0.012% saponin and 7% horse serum (Invitrogen) for 30 min at RT. Staining with primary antibodies was performed in IF buffer containing 0.012% saponin and 5% horse serum either overnight at 4°C or for 2 h at RT followed by incubation with secondary antibodies for 60 min at RT. After washing cells were mounted in Prolong-Gold anti-fading reagent (Molecular Probes) and were analyzed using confocal laser-scanning microscope LSM 510 (Zeiss, Oberkochen, Germany). Images were taken using 63x oil immersion objective lense. Quantitative analysis of the degree of the co-localization/overlay were measured using Carls Zeiss LSM 510 Image examiner Software between two channels.

Electron microscopy

BMMC were fixed in 1.5% glutaraldehyde (Serva) diluted in 0.1 M cacodylate buffer pH 7.4 stored for 20 minutes at room temperature, post-fixed in 1% OsO_4 for 60 minutes at 4°C, dehydrated in ethanol, and finally embedded in Dow Epoxy Resin (DER 332, Unione Chimica Europea, Milano, Italy). For double immunogold labelling of RPMC, ultrathin sections, cut by an ultramicrotome Ultracut UCT; Leica (Wien, Austria) were mounted on nickel grids etched for one min with 1% periodic acid and rinsed in distilled water. Grids with the section sides facing downward were incubated in 20 mM Tris-HCl pH 8.2, containing 2% BSA, 1% goat serum, 0.05% tween-20, 0.1% Triton X-100 and

exposed overnight at 4°C to rabbit anti-VAMP-8 diluted 1:20 in the same buffer. Grids were washed in 20 mM Tris-HCl pH 8.2 containing NaCl 225 mM, 2 mM NaN3, 0.05% tween-20, 0.5% BSA, 0.1% Triton X-100, 0.5% goat serum and were incubated thereafter one h at room temperature with 10 nm gold-conjugated goat anti-rabbit (British Biocell International; Cardiff, UK) diluted 1:50 in Tris-HCl-BSA-Triton. Grids were rinsed, turned over with the section sides facing upward, according to Bendayan [31] and exposed to undiluted rabbit anti-Serotonin. The procedure followed thereafter was as above with the exception that 20nm gold-conjugated Protein A-G (British Biocell International) diluted 1:50 in Tris-HCl-BSA-Triton was used as revealing system. Sections were analysed by transmission electron microscope (EM208 Philips, Eindhoven, Netherland). Micrographs were taken with a Morada camera (Olympus Soft Imaging Solution (OSIS), Muenster, Germany). Control experiments using normal rabbit and mouse IgG were performed in parallel. Background of gold particles found on the granule surface was 2.8 % and within the granule matrix was 4.8 % (SG counted: n = 426 and 602 for specific and control staining, respectively)

Statistical analysis

Statistical analysis was performed with Origin Pro 7.5 Software. For *in vivo* data, a paired Student's t test was used. For comparing responses of the mutant cells, a one-way Anova test was used, as indicated.

Results

Mast cell development is unaffected in VAMP-8-deficient mice

The role of VAMP-8 in mast cell secretory events was examined using VAMP-8-deficient mice generated via a gene knockout approach [27]. We first verified the absence and presence of VAMP-8 protein in BMMCs derived from VAMP-8-deficient and WT mice, respectively. Fig. 1A shows that VAMP-8 is highly expressed in WT BMMCs like in the

MCP-5 murine mast cell line and in kidney extracts used as a control [23] while VAMP-8-deficient BMMCs lack expression as in brain [24]. We also examined whether deficiency of VAMP-8 affects mast cell development and tissue distribution. Analysis of toluidine blue stained sections from ear, skin and tongue revealed no significant differences in mast cell numbers between WT and VAMP-8-deficient mice (Fig. 1B). Light and electron microscopy examination of cell morphology and granular appearance did not show any differences in mast cells isolated from the peritoneum (Fig. 1C)**.** In cultured BMMCs we also did not find any evidences for gross morphological alterations as well as differences in the number of intracellular granules although WT BMMCs contain a slight but significantly higher proportion of immature granules containing no or little electron-dense material (Fig. S1 and Table 1). BMMCs did, however, contain similar amounts of intragranular histamine on a per cell basis (32.6 ± 3.4 pM/cell and 29.1 ± 5.3 pM/cell) in WT versus VAMP-8-deficient cells and they expressed similar levels of the mast cell-specific surface markers c-kit and FcεRI (Fig. 1D).

VAMP-8-deficient mast cells show impaired degranulation responses *in vitro* and *in vivo*

We have reported earlier that in the RBL mast cell line VAMP-8 co-localized with SGs [18]. This suggested that VAMP-8 might be involved in the fusion events during degranulation. To examine this issue directly we measured release of the granular-stored enzyme β-hexosaminidase in VAMP-8-deficient BMMCs after stimulation through FcεRI. Cells were sensitized with anti-DNP IgE and subsequently stimulated with DNP-HSA in dose response (Fig. 2A) and kinetic (Fig. 2B) experiments. Release of β-hexosaminidase was optimal at a dose of antigen around 10 ng/ml reaching maximal levels by 9 min. Relative to WT BMMCs, the degranulation of VAMP-8-deficient BMMCs was markedly inhibited. We also determined release of histamine, a major mediator of

allergic inflammation and vasodilation that is specifically stored in mast cell SGs [2,4]. Fig 2C shows that similar to β-hexosaminidase, the kinetics of histamine release was decreased in VAMP-8-deficient BMMCs as compared to WT BMMCs. These data indicated that VAMP-8-deficient mast cells show a marked deficit in their capacity to release prestored mediators from their SGs.

To test the impact of VAMP-8 deficiency on the allergic response, *in vivo*, we analyzed the responsiveness of WT and VAMP-8-deficient mice in a passive systemic anaphylaxis experiment. Passive systemic anaphylaxis by IgE antibodies largely depends on mast cells, which rapidly release histamine and serotonin resulting in locally increased blood vessel permeability [2,32,33]. Mice were primed by i.v. injection of purified monoclonal anti-DNP IgE antibody and 24 h later animals were challenged i.v. with DNP–HSA. The level of blood plasma histamine was determined 2 min after antigen challenge. VAMP-8-deficient mice showed reduced levels of histamine as compared to WT mice (Fig. 2D). A similar inhibition was confirmed in another set of experiments where histamine levels were determined 60 min after antigen challenge ($p < 0.001$, $n=9$). No significant amounts of histamine were observed in mice challenged with vehicle (not shown).

VAMP-8-deficient mast cells are not impaired in cytokine/chemokine production

Another consequence of FcεRI engagement is the production of pro-inflammatory cytokines such as IL-6, TNF and the chemokine macrophage inflammatory protein 1α (MIP-1α) [2]. We analyzed FcεRI-induced secretion of TNF, IL-6 and MIP-1α into the medium in WT and VAMP-8-deficient BMMCs. Our analysis revealed that no significant amounts of TNF, IL-6 and MIP-1α were released by short term stimulation (< 30 min), indicating that little or undetectable amounts of these cytokines are contained in rapidly mobilized SGs under our culture conditions. We also could not detect cytokine production in the absence of antigen stimulation demonstrating that the cells did not

release spontaneously the cytokines tested within an 8 h period (not shown). Cross-linking the receptor induced, however, the secretion of significant amounts of TNF, IL-6 and MIP-1α into the culture medium in a time-dependent manner. Maximal secretion was achieved between 1 to 2 h. and no significant differences in cytokine release were observed between WT and VAMP-8-deficient BMMCs (Fig 3). These BMMCs also released IL-4 upon stimulation albeit at very low levels (~60 pg/ml) but no differences were seen between WT and VAMP-8-deficient BMMCs (not shown). Therefore, VAMP-8 deficiency impairs FcεRI-induced degranulation but not cytokine and chemokine secretion.

Role of VAMP-8 in membrane fusion

To further examine the role of VAMP-8 in the molecular events leading to mast cell degranulation, we explored whether deficiency of VAMP-8 alters the expression of other SNAREs that could be involved in granule fusion. Fig 4A shows that no significant differences were observed for several membrane trafficking proteins including syntaxin-2, -3, -4, SNAP-23, VAMP-2, VAMP-3, VAMP-4 and the accessory protein Munc18-2.

Given that VAMPs are known to function in the fusion process of SGs, a presumed late step in mast cell activation, we investigated any possible alterations in signaling events upstream of degranulation and cytokine production in WT and VAMP-8-deficient BMMCs. Our results (Fig. S2) revealed that early signaling events (phosphorylation of Syk, p38, p42-44ERK and AKT) were not altered by VAMP-8-deficiency. The results differed, however, when the early receptor-stimulated signalling events were by-passed using PMA/ionomycin or thapsigargin. Fig 4B shows that both stimuli readily mobilized cytoplasmic granules for β-hexosaminidase release in WT cells. In contrast, as was the case for FcεRI-induced stimulation, release was markedly inhibited in VAMP-8-deficient BMMCs as compared to WT cells. Again, no differences were seen when

PMA/ionomycin-induced MIP-1α production was examined (not shown). These data clearly demonstrate a role for VAMP-8 in a late step of SG exocytosis of preformed mediators, while early signalling events and other late events such as release of newly synthesized cytokines were not affected.

The collective findings above suggested that FcεRI-stimulation involved a VAMP-8-dependent fusion mechanism and SNARE complex formation during degranulation. To test this directly, we examined whether VAMP-8 formed complexes with other SNARE partners upon cell activation. IgE-sensitized BMMC were either left unstimulated or were stimulated with DNP-HSA. To stabilize interactions among SNARE proteins, N-ethylmaleimide (NEM), a sulfhydryl-alkylating agent known to inactivate NSF and block SNARE disassembly and mast cell exocytosis, was added after stimulation [18,34]. SNAP-23 and syntaxin-4 were then immunoprecipitated and associated VAMP-8 was evaluated by immunoblot analysis. Fig 4C (left panels) shows that little or no VAMP-8 was detected in a complex with SNAP-23 or syntaxin-4 in unstimulated cells. Following stimulation, an increase in the amount of VAMP-8 co-precipitating with SNAP-23 or syntaxin-4 was observed. Quantitative analysis (Fig. 4C, right panels) showed that complex formation peaked between 1 and 3 min indicating that SNARE complex formation was modulated by stimulation. As expected, no association was observed in VAMP-8-deficient BMMCs (Fig. 4C). We also analyzed SNARE complex formation of SNAP-23 with VAMP-2 (Fig. 4D). Little SNAP-23-VAMP-2 complexes were observed in unstimulated cells. They did not change significantly in stimulated WT BMMCs, while in VAMP-8-deficient BMMCs they showed a tendency to increase indicating some possible compensatory effects.

Analysis of intracellular compartments important in degranulation and TNF production

To gain further insight on the role of VAMP-8 in granule mobilization, we analyzed whether VAMP-8 localizes to SGs by assessing the colocalization with the SG marker serotonin in WT BMMCs. Similar to the data obtained in the RBL mast cells [18], a fraction of VAMP-8 protein overlapped with granule serotonin (Mean ± SD: 34.1 ± 12.1%, rat anti-serotonin and 30.3 ± 8.3 %, mo anti-serotonin)**,** however, some compartments appeared to have only VAMP-8 or serotonin (Fig. 5A upper panel). Partial overlap (34.3 ± 11.8 %) was also seen with mMCP-6 as a SG marker (Fig 5A lower panel). We also analyzed VAMP-8 localization at the ultrastructural level by immunoelectron microscopy using RPMC that have a highly differentiated secretory granule compartment. Only weak staining for serotonin (20 nm GP) was seen with occasionally a detectable GP within secretory granules (Fig 5B). Staining for VAMP-8 (10 nm GP) was somewhat more prominent and was often observed at the surface of secretory granules. Interestingly, VAMP-8 was sometimes also detected inside. Closer inspection (see inset, Fig. 5B) indicated that it might locate to vesicular-like structures resembling multivesicular bodies or remnants derived thereof [35]. We next investigated the localisation of VAMP-8 in stimulated cells versus unstimulated cells using confocal analysis. In agreement with a multigranular mode of exocytosis [36], our confocal analysis demonstrated that stimulation using calcium ionophore induced a coalescence of VAMP-8 and serotonin-containing vesicular structures with an increase in co-localisation and relocation to the cell periphery as can be seen in comparison to the staining with the plasma membrane marker c-kit (Fig. 5C and Fig. S3A for quantitative analysis). A similar increase in colocalisation between VAMP-8 and serotonin as well as VAMP-8 and mMCP-6 was also observed after IgE-dependent stimulation) when compared to PMA/ionomycin-induced stimulation (Fig. S3B and C). The confocal images corresponding to IgE-stimulated cells are shown in Fig. S4. As VAMP-8-deficient cells cannot be analyzed by VAMP-8 staining, we examined in parallel WT and VAMP-8-deficient BMMCs using

syntaxin-3 as a SG marker. As shown previously [30], in unstimulated cells syntaxin-3 has a uniform granular distribution that co-localized with serotonin in both types of cells and thus may have a role in granule-granule fusion (Fig. 6A). Syntaxin-3 showed a somewhat higher co-localisation with serotonin in VAMP-8-deficient BMMCs. However, in agreement with a defective fusion mechanism, colocalisation of syntaxin-3 and serotonin did not increase after stimulation with calcium ionophore in VAMP-8-deficient BMMCs and syntaxin-3 appeared to relocate less extensively to the cell periphery when compared to WT cells (Fig. 6B and Fig S3D).

Since no differences in cytokine secretion were found between WT and VAMP-8-deficient cells, we also analyzed trafficking of TNF. In agreement with the absence of release after short-term stimulation, no TNF staining was detectable in unstimulated cells (Fig 7A). To enable detection after stimulation, cells were treated with TNF-alpha converting enzyme (TACE) inhibitor TAPI-1, which prevents cleavage of the membrane-bound precursor of TNF into the mature secreted form once it has reached the surface. Upon such treatment significant amounts of TNF accumulated at the cell periphery in cells stimulated for 3 h with IL-1β (Fig. 7B). The latter has been shown to be a potent inducer of cytokine/chemokine release in mast cells in the absence of degranulation [37]. By contrast, staining of TNF after stimulation with PMA/ionomycin was very weak (not shown). Analysis of VAMP-8-containing compartments showed that after the 3 h stimulation period VAMP-8 was largely intracellular and does not substantially redistribute to the periphery in conformity with the absence of degranulation under these stimulation conditions. VAMP-8 also did not considerably co-localize with the TNF found at the cell periphery (mean ± SD; 16.1 ± 10.7,). By contrast, staining of cells with VAMP-3 revealed large patches of vesicular-like structures at the periphery sometimes extending into ruffle-like projections and a strong overlap with TNF both in WT and in VAMP-8-deficient BMMCs (mean ± SD; 52.3 ± 10.1 and 51.3 ± 14.7, respectively). This

is in agreement with the lack of effect of VAMP-8 on cytokine secretion. These results suggest that the terminal trafficking step of TNF release and processing in mast cells similar to macrophages [6] may include VAMP-3-containing vesicular compartments.

Discussion

In the present study we demonstrate in mast cells that the v-SNARE VAMP-8 functions in the exocytosis of granular stored inflammatory mediators, but does not play a role in the exocytosis of newly synthesized cytokines/chemokines. I*n vitro* experiments demonstrated an about 50 % inhibition in IgE-stimulated release of β-hexosaminidase and histamine in VAMP-8-deficient mast cells. These results were confirmed in passive systemic anaphylaxis experiments where a similar reduction in blood plasma histamine levels known to depend on the activation of mast cells [32,33] was noted. By contrast, the secretion of TNF, IL-6 and MIP-1α was not affected by the absence of VAMP-8.

These results place VAMP-8 as a fusion protein that segregates preformed mediator release from cytokine/chemokine molecular trafficking pathways in mast cells. Previous studies have shown that mast cell SGs are secretory lysosomes with a close connection between the secretory and endocytic pathway [8-10,35]. Three types of SGs have been identified [35]: i) type I granules, which contain multivesicular bodies, are accessible to endocytoc tracers and devoid of serotonin, ii) type II SGs composed of both multivesicular bodies and electron dense material, are accessible to endocytic tracers and positive for serotonin and iii) type III SGs containing only electron dense material, positive for serotonin but are inaccessible to endocytotic tracers. VAMP-8 was originally characterized as a v-SNARE connected to endocytotic and endosomal-lysosomal molecular trafficking [24-26]. More recently it was also shown to function in granule exocytosis in exocrine cells and platelets [27,28]. In agreement with the connection between

endocytic and exocytic pathways we found an overlap of VAMP-8 and serotonin and MCP-6 containing secretory granules in BMMC using confocal analysis similar to the results with tumor mast cells [18]. The overlap was partial for both markers, which can be explained by the above described heterogeneity of the granular compartment and previous data showing that VAMP-8 also localizes to endosomes [25]. In immunoelectronmicroscopy analysis besides on the granule membrane it was also sometimes found in intracellular structures that could be endosomal-derived multivesicular bodies or remnants derived thereof [35]. It is also in agreement with our data showing that release was not inhibited completely, neither *in vitro* nor *in vivo*. Thus, besides VAMP-8 other v-SNAREs may also be operative. Possible candidates are VAMP-2 and VAMP-7 as both proteins partially colocalize with SGs in mast cells [18] and exogenously expressed fluorescent-tagged forms of these SNAREs relocated to the cell periphery upon stimulation [20,38].

Biochemical evidence also supports the direct implication of VAMP-8 in fusion during degranulation. Initial experiments showed that absence of VAMP-8 had no effect on expression levels of other trafficking proteins differing from the report in platelets where some compensatory effects were observed [28]. Furthermore, in addition to IgE-stimulated release, ionomycin or thapsigargin-initiated release was also inhibited placing VAMP-8 at a late step likely situated at the level of fusion. Indeed, we demonstrated that VAMP-8 within 1-3 minutes forms complexes with both SNAP-23 and syntaxin-4 in WT but not VAMP-8-deficient BMMCs. As SNAP-23 and syntaxin-4 were previously implicated in SG fusion in mast cells [17,18] our data strongly support the role of VAMP-8 in fusion. We also detected complexes between SNAP-23 and VAMP-2. In VAMP-8-deficient BMMCs they showed a tendency to increase upon stimulation while this was less the case in WT BMMCs supporting our statement above that VAMP-2 may also play a role or compensate for the loss of VAMP-8 in SG fusion events.

The direct implication of VAMP-8 in the membrane fusion during degranulation was further supported by our data showing that it relocated to the periphery in stimulated cells similar to syntaxin-3, another marker for SGs in mast cells. Interestingly, colocalization between VAMP-8 and serotonin increased in short-term stimulated cells (where serotonin was still detectable) suggesting that degranulation may involve additional fusion events, such as recently proposed for secretory lysosomal exocytosis in cytotoxic T cells. In these cells cytotoxic vesicles become primed for exocytosis after interaction with a Munc13-4/Rab27a positive "exocytic vesicle" [11]. Interestingly, both Munc13-4 and Rab27b, a Rab27a homologue have recently been described to play a role in mast cell degranulation [39,40] and similar mechanisms may therefore also be operative in mast cells. In VAMP-8-deficient BMMCs somewhat more overlap between syntaxin-3 and serotonin was observed. This relates to our EM data showing that VAMP-8-deficient BMMCs contain more mature granules (Table 1). However, in agreement with the inhibition of degranulation observed in these cells no increase in colocalisation became apparent in stimulated cells and relocation of syntaxin-3 to the PM was less prominent as compared to WT BMMCs.

With the notable exception of TNF, which can be found at least in part in cytoplasmic granules in some types of mast cells [41-43], secretion of cytokines/chemokines depends on protein synthesis and subsequent secretion by a still ill-defined intracellular trafficking pathway. Cytokines/chemokine in mast cells are released by various stimuli in the absence of degranulation [37,44,45] suggesting that their trafficking pathways are different. Our data demonstrate that absence of VAMP-8 does not affect TNF, IL-6, IL-4 and MIP-1α secretion from BMMCs supporting that cytokine secretion does not use the secretory lysosomal pathway defined by VAMP-8. Cytokine trafficking has been difficult to study, likely due to the transient nature of the trafficking events. In agreement, only addition of a TNF converting enzyme inhibitor that blocks proteolytic release of plasma membrane

exposed cytokine allowed to visualize some protein after stimulation with ionomycin or thapsigargin. This was further enhanced when cells were stimulated with IL-1β, which does not induce degranulation. It is possible that proteases released by degranulation may elicit nonspecific cleavage of unprocessed surface exposed TNF [46], while this may be less the case after degranulation-independent activation with IL-1β. Comparative analysis of unprocessed TNF with VAMP-8-containing compartments showed that after 3 h of stimulation, VAMP-8 was largely intracellular and does not substantially redistribute to the cell periphery in conformity with the absence of degranulation under these stimulation conditions. VAMP-8 also did not considerably co-localize with surface exposed TNF. We therefore looked at VAMP-3, previously reported to traffic from the Golgi to recycling endosomes, where it mediates release into the phagocytic cup [6]. Interestingly, although mast cell secretory events and not phagocytosis were examined we found that surface exposed TNF concentrated at the periphery together with VAMP-3-positive compartments that sometimes extended into ruffle-like projections. This indicates that TNF trafficking in mast cells similar to macrophages may involve VAMP-3-positive compartments. As VAMP-3 has previously been associated with the endocytotic recycling compartment this could indicate interception with a constitutive intracellular trafficking pathway [6]. However, further functional studies are necessary to elucidate whether VAMP-3 may be involved in regulated fusion events.

Taken together, the present findings demonstrate an important role for VAMP-8, a v-SNARE originally localized to endosomes and lysosomes, in mast cell degranulation. A role for VAMP-8 in exocytosis has also be demonstrated in the exocrine system [27,28]. Together with recent data, which show a role for VAMP-8 in lysosomal granules exocytosis in platelets [28], the evolving view is that regulated exocytosis of secretory lysosomes in hematopoietic cells may generally depend on VAMP-8 as one of the major

v-SNAREs involved in fusion. These findings extend the role of VAMP-8 as a specific regulator of secretory lysosomal exocytosis. It further demonstrates the intimate connection between endosomal and secretory pathways in these cells. Our results show that VAMP-8 does not affect cytokine release indicating that cytokine trafficking uses distinct trafficking pathways independent of VAMP-8. For TNF, as observed in macrophages [6,7], this may involve a VAMP-3 containing recycling compartment. This distinction of VAMP-3-containing cytokine-occupied vesicular-like structures versus VAMP-8-containing SGs affords the possibility that interference with intracellular trafficking pathways regulated by VAMP-8 and possibly other fusion proteins might represent a specific therapeutic strategy to selectively interfere with degranulation, but not cytokine release in mast cells. However, side effects on other exocrine pathways that involve VAMP-8 such as secretion from pancreatic acinar cells have to be considered [27]. The utility of this approach would be to ameliorate immediate hypersensitivity while keeping intact some of the innate immune function of the mast cell.

Acknowledgements

NT and UB were supported by the Fondation de Recherche Médicale (program *Défis de la Recherche en Allergologie*). The research project of UB and CB has been supported by a Marie Curie Early Stage Research Training Fellowship of the European Community's Sixth Framework Programme under contract number 504926. We thank Cécile Pouzet and Samira Benadda (IFR 02, Paris-Nord) for the help with confocal image acquisition. The research of JR is supported by the intramural research program of the National Institute of Arthritis and Musculoskeletal and Skin Diseases, National Institutes of Health. We also thank Hwee Chien Liew and Jie Li for technical assistance. We also thank Dr. Lisa Scandiuzzi, Dr. Meetu Tiwari and Dr. Renato C. Monteiro for critical and thoughtful discussions.

Author contributions

N.T. performed most of the experiments and analyzed the data and wrote manuscript; C-C.W. performed experiments and analyzed the data. C.B. performed experiments and analyzed the data. G.K. performed in vivo experiments, F.V. and M.R.S. performed EM studies and analysis. Z. Q. performed histological analysis. J.R. provided critical reagents, helped with data analysis and participated in manuscript writing. G. Z. designed experiments and analyzed data. W. H. supervised experiments iand participated in study design. U.B. designed the study, analyzed data and wrote manuscript.

Conflict of Interest Disclosure

The authors declare no competing financial interests.

References

1. Metcalfe DD, Baram D, Mekori YA. Mast cells. Physiol Rev. 1997;77:1033-1079

2. Galli SJ, Kalesnikoff J, Grimbaldeston MA, Piliponsky AM, Williams CM, Tsai M. Mast cells as "tunable" effector and immunoregulatory cells: recent advances. Annu Rev Immunol. 2005;23:749-786

3. Grimbaldeston MA, Metz M, Yu M, Tsai M, Galli SJ. Effector and potential immunoregulatory roles of mast cells in IgE-associated acquired immune responses. Curr Opin Immunol. 2006;18:751-760

4. Blank U, Rivera J. The ins and outs of IgE-dependent mast-cell exocytosis. Trends Immunol. 2004;25:266-273

5. Klemm S, Gutermuth J, Hultner L, Sparwasser T, Behrendt H, Peschel C, Mak TW, Jakob T, Ruland J. The Bcl10-Malt1 complex segregates Fc epsilon RI-mediated nuclear factor kappa B activation and cytokine production from mast cell degranulation. J Exp Med. 2006;203:337-347

6. Murray RZ, Kay JG, Sangermani DG, Stow JL. A role for the phagosome in cytokine secretion. Science. 2005;310:1492-1495

7. Stow JL, Manderson AP, Murray RZ. SNAREing immunity: the role of SNAREs in the immune system. Nat Rev Immunol. 2006;6:919-929

8. Xu K, Williams RM, Holowka D, Baird B. Stimulated release of fluorescently labeled IgE fragments that efficiently accumulate in secretory granules after endocytosis in RBL-2H3 mast cells. J Cell Sci. 1998;111:2385-2396.

9. Baram D, Adachi R, Medalia O, Tuvim M, Dickey BF, Mekori YA, Sagi-Eisenberg R. Synaptotagmin II negatively regulates Ca2+-triggered exocytosis of lysosomes in mast cells. J Exp Med. 1999;189:1649-1658

10. Andrews NW. Regulated secretion of conventional lysosomes. Trends Cell Biol. 2000;10:316-321

11. Menager MM, Menasche G, Romao M, Knapnougel P, Ho CH, Garfa M, Raposo G, Feldmann J, Fischer A, de Saint Basile G. Secretory cytotoxic granule maturation and exocytosis require the effector protein hMunc13-4. Nat Immunol. 2007;8:257-267

12. Haberman Y, Ziv I, Gorzalczany Y, Hirschberg K, Mittleman L, Fukuda M, Sagi-Eisenberg R. Synaptotagmin (Syt) IX is an essential determinant for protein sorting to secretory granules in mast cells. Blood. 2007;109:3385-3392

13. Humphries DE, Wong GW, Friend DS, Gurish MF, Qiu WT, Huang C, Sharpe AH, Stevens RL. Heparin is essential for the storage of specific granule proteases in mast cells. Nature. 1999;400:769-772

14. Forsberg E, Pejler G, Ringvall M, Lunderius C, Tomasini-Johansson B, Kusche-Gullberg M, Eriksson I, Ledin J, Hellman L, Kjellen L. Abnormal mast cells in mice deficient in a heparin-synthesizing enzyme. Nature. 1999;400:773-776

15. Abrink M, Grujic M, Pejler G. Serglycin is essential for maturation of mast cell secretory granule. J Biol Chem. 2004;279:40897-40905

16. Jahn R, Scheller RH. SNAREs--engines for membrane fusion. Nat Rev Mol Cell Biol. 2006;7:631-643

17. Guo Z, Turner C, Castle D. Relocation of the t-SNARE SNAP-23 from lamellipodia-like cell surface projections regulates compound exocytosis in mast cells. Cell. 1998;94:537-548

18. Paumet F, Le Mao J, Martin S, Galli T, David B, Blank U, Roa M. Soluble NSF attachment protein receptors (SNAREs) in RBL-2H3 mast cells: functional role of syntaxin 4 in exocytosis and identification of a vesicle-associated membrane protein 8-containing secretory compartment. J Immunol. 2000;164:5850-5857

19. Vaidyanathan VV, Puri N, Roche PA. The last exon of SNAP-23 regulates granule exocytosis from mast cells. J Biol Chem. 2001;276:25101-25106.

20. Hibi T, Hirashima N, Nakanishi M. Rat basophilic leukemia cells express syntaxin-3 and VAMP-7 in granule membranes. Biochem Biophys Res Commun. 2000;271:36-41.

21. Olszewski MB, Groot AJ, Dastych J, Knol EF. TNF trafficking to human mast cell granules: mature chain-dependent endocytosis. J Immunol. 2007;178:5701-5709

22. Olszewski MB, Trzaska D, Knol EF, Adamczewska V, Dastych J. Efficient sorting of TNF-alpha to rodent mast cell granules is dependent on N-linked glycosylation. Eur J Immunol. 2006;36:997-1008

23. Wang CC, Shi H, Guo K, Ng CP, Li J, Qi Gan B, Chien Liew H, Leinonen J, Rajaniemi H, Hong Zhou Z, Zeng Q, Hong W. VAMP8/Endobrevin as a General Vesicular SNARE for Regulated Exocytosis of the Exocrine System. Mol Biol Cell. 2007;18:1056-1063

24. Antonin W, Holroyd C, Tikkanen R, Honing S, Jahn R. The R-SNARE Endobrevin/VAMP-8 mediates homotypic fusion of early endosomes and late endosomes [In Process Citation]. Mol Biol Cell. 2000;11:3289-3298

25. Wong SH, Zhang T, Xu Y, Subramaniam VN, Griffiths G, Hong W. Endobrevin, a novel synaptobrevin/VAMP-like protein preferentially associated with the early endosome. Mol Biol Cell. 1998;9:1549-1563

26. Mullock BM, Smith CW, Ihrke G, Bright NA, Lindsay M, Parkinson EJ, Brooks DA, Parton RG, James DE, Luzio JP, Piper RC. Syntaxin 7 is localized to late endosome compartments, associates with Vamp 8, and Is required for late endosome-lysosome fusion. Mol Biol Cell. 2000;11:3137-3153

27. Wang CC, Ng CP, Lu L, Atlashkin V, Zhang W, Seet LF, Hong W. A role of VAMP8/endobrevin in regulated exocytosis of pancreatic acinar cells. Dev Cell. 2004;7:359-371

28. Ren Q, Barber HK, Crawford GL, Karim ZA, Zhao C, Choi W, Wang CC, Hong W, Whiteheart SW. Endobrevin/VAMP-8 is the primary v-SNARE for the platelet release reaction. Mol Biol Cell. 2007;18:24-33

29. Mallard F, Tang BL, Galli T, Tenza D, Saint-Pol A, Yue X, Antony C, Hong W, Goud B, Johannes L. Early/recycling endosomes-to-TGN transport involves two SNARE complexes and a Rab6 isoform. J Cell Biol. 2002;156:653-664

30. Martin-Verdeaux S, Pombo I, Iannascoli B, Roa M, Varin-Blank N, Rivera J, Blank U. Analysis of Munc18-2 compartmentation in mast cells reveals a role for microtubules in granule exocytosis. J. Cell Sci. 2003;116:325-334

31. Bendayan M. Double immunocytochemical labeling applying the protein A-gold technique. J Histochem Cytochem. 1982;90:81-85

32. Miyajima I, Dombrowicz D, Martin TR, Ravetch JV, Kinet JP, Galli SJ. Systemic anaphylaxis in the mouse can be mediated largely through IgG1 and Fc gammaRIII. Assessment of the cardiopulmonary changes, mast cell degranulation, and death associated with active or IgE- or IgG1-dependent passive anaphylaxis. J Clin Invest. 1997;99:901-914

33. Finkelman FD, Rothenberg ME, Brandt EB, Morris SC, Strait RT. Molecular mechanisms of anaphylaxis: lessons from studies with murine models. J Allergy Clin Immunol. 2005;115:449-457; quiz 458

34. Puri N, Kruhlak MJ, Whiteheart SW, Roche PA. Mast cell degranulation requires N-ethylmaleimide-sensitive factor-mediated SNARE disassembly. J Immunol. 2003;171:5345-5352

35. Raposo G, Tenza D, Mecheri S, Peronet R, Bonnerot C, Desaymard C. Accumulation of major histocompatibility complex class II molecules in mast cell secretory granules and their release upon degranulation. Mol Biol Cell. 1997;8:2631-2645

36. Alvarez de Toledo G, Fernandez J. Compound versus multigranular exocytosis in peritoneal cells. J. Gen. Physiol. 1990;95:397-402

37. Kandere-Grzybowska K, Letourneau R, Kempuraj D, Donelan J, Poplawski S, Boucher W, Athanassiou A, Theoharides TC. IL-1 induces vesicular secretion of IL-6 without degranulation from human mast cells. J Immunol. 2003;171:4830-4836

38. Miesenbock G, De Angelis DA, Rothman JE. Visualizing secretion and synaptic transmission with pH-sensitive green fluorescent proteins. Nature. 1998;394:192-195

39. Neeft M, Wieffer M, de Jong AS, Negroiu G, Metz CH, van Loon A, Griffith J, Krijgsveld J, Wulffraat N, Koch H, Heck AJ, Brose N, Kleijmeer M, van der Sluijs P. Munc13-4 is an effector of rab27a and controls secretion of lysosomes in hematopoietic cells. Mol Biol Cell. 2005;16:731-741

40. Mizuno K, Tolmachova T, Ushakov DS, Romao M, Abrink M, Ferenczi MA, Raposo G, Seabra MC. Rab27b regulates mast cell granule dynamics and secretion. Traffic. 2007;8:883-892

41. Gordon JR, Galli SJ. Mast cells as a source of both preformed and immunologically inducible TNF-alpha/cachectin. Nature. 1990;346:274-276

42. Gordon JR, Galli SJ. Release of both preformed and newly synthesized tumor necrosis factor alpha (TNF-alpha)/cachectin by mouse mast cells stimulated via the Fc epsilon RI. A mechanism for the sustained action of mast cell-derived TNF-alpha during IgE-dependent biological responses. J. Exp. Med. 1991;174:103-107

43. Beil WJ, Login GR, Aoki M, Lunardi LO, Morgan ES, Galli SJ, Dvorak AM. Tumor necrosis factor alpha immunoreactivity of rat peritoneal mast cell granules decreases during early secretion induced by compound 48/80: an ultrastructural immunogold morphometric analysis. International Archives of Allergy & Immunology. 1996;109:383-389

44. Fischer M, Harvima IT, Carvalho RF, Moller C, Naukkarinen A, Enblad G, Nilsson G. Mast cell CD30 ligand is upregulated in cutaneous inflammation and mediates degranulation-independent chemokine secretion. J Clin Invest. 2006;116:2748-2756

45. Allakhverdi Z, Comeau MR, Jessup HK, Yoon BR, Brewer A, Chartier S, Paquette N, Ziegler SF, Sarfati M, Delespesse G. Thymic stromal lymphopoietin is released by human epithelial cells in response to microbes, trauma, or inflammation and potently activates mast cells. J Exp Med. 2007;204:253-258

46. Zhao W, Oskeritzian CA, Pozez AL, Schwartz LB. Cytokine production by skin-derived mast cells: endogenous proteases are responsible for degradation of cytokines. J Immunol. 2005;175:2635-2642

Figure Legends

Figure 1. Development of mast cells is not affected in VAMP-8-deficient mice

(A) VAMP-8 expression levels in tissue homogenates of brain, kidney, murine MCP-5 mast cells, VAMP-8-deficient and WT BMMCs using anti-VAMP-8. Blots were stripped and reprobed with anti-actin. (B) Representative toludine blue staining of ear and tongue cross-sections (upper panel) showing the distribution of tissue mast cells (arrowheads) in VAMP-8-deficient and WT mice (40 x obj). (lower panel) Corresponding quantitative enumeration of mast cells in ear, tongue, and abdominal skin sections (3 mice/genotype). Data are mean ± SEM derived from 5 high power field counted/mouse. No significant difference among VAMP-8-deficient and WT mice were observed. (C) Representative toludine blue staining (upper panel) and ultrastructural analysis (lower panel) by electron microscopy (original magnification x 13,500) of mouse peritoneal mast cells from VAMP-8-deficient and WT mice. (D) Expression of FcεRI and c-kit on BMMCs from VAMP-8-deficient and WT mice. Continuous and dotted lines represent VAMP-8-deficient and WT BMMCs, respectively as compared to isotype control (dark area).

Figure 2. Defective degranulation and passive systemic anaphylactic responses in VAMP-8-deficient BMMCs and mice

VAMP-8-deficient and WT BMMCs sensitized overnight with anti-DNP IgE were stimulated for 30 min with the indicated concentrations of DNP–HSA (A) or for indicated time points using 10 ng/ml (B) and release of β-hexosaminidase was determined. (C) VAMP-8-deficient and WT BMMCs were sensitized with IgE before stimulation with 10 ng/ml DNP–HSA and release of histamine was determined. Data (percent release ± SEM) are from three individual experiments and are representative of 4, 5 and 2 in A, B and C, respectively. All differences were significant ($p < 0.01$) and were determined by one way ANOVA. (D) In vivo passive systemic anaphylactic challenge of VAMP-8-

deficient and WT mice. Mice (n=7) were passively sensitized i.v. with 30µg purified IgE-anti-DNP and were challenged 24 h later with 100 µg DNP-HSA. After 2 min blood plasma was collected and plasma histamine concentrations were determined by ELISA.

Figure 3. Cytokine release is not affected in VAMP-8-deficient BMMCs.

VAMP-8 +/+ and VAMP-8 -/- BMMCs were sensitized overnight with anti-DNP IgE and stimulated with 10ng/ml DNP–HSA for the indicated times. Supernatants were collected, and TNF, IL-6 and MIP-1α protein concentrations were determined by ELISA. Data are means ± SEM from triplicate samples derived from three different BMMC cultures and are representative of five independent experiments.

Figure 4. VAMP-8 acts at a late fusion step in the mast cell degranulation response.

(A) The level of SNARE and SNARE-related proteins in VAMP-8-deficient and WT BMMCs were analyzed. An equivalent of 2×10^5 BMMCs per lane were migrated on SDS-PAGE and analyzed by western blotting using indicated specific abs. (B) VAMP-8-deficient and WT BMMCs were stimulated with either thapsigargin (1µM) or ionomycin/PMA (500nM/20nM) for 10 min and percent release of β-hexosaminidase was determined. Data are means ± SEM from triplicate samples derived from three different BMMC cultures and are representative of three independent experiments. ** $P < 0.05$ by one way ANOVA. (C) Enhanced association of SNAP23 and syntaxin-4 with VAMP-8 after stimulation. IgE-sensitized indicated BMMCs (10^7) were either left unstimulated (NS) or were stimulated (S) with 10ng/ml DNP-HSA for indicated times followed by NEM treatment as described in methods. Immunoprecipitation was performed with indicated abs followed by immunoblotting with anti-VAMP-8. Blots were then stripped and reprobed with abs to either syntaxin-4 or SNAP-23 as indicated. Corresponding quantitative analysis is shown to the right (n= 3, ** $p < 0.05$). (D) VAMP-8-deficient BMMCs show a tendency to increased complex formation with SNAP-23 in stimulated

BMMCs. IgE-sensitized indicated BMMCs (10^7) were treated as above. Immunoprecipitation was performed with SNAP-23 abs followed by immunoblotting with anti-VAMP-2. For loading control blots were cut into two parts and probed with SNAP-23 as indicated. Corresponding quantitative analysis is shown to the right (n= 3).

Figure 5. **Localisation of VAMP-8 and SGs markers in resting and stimulated WT BMMCs**

(A) Colocalization of VAMP-8 with the SG markers serotonin and mMCP-6 were analyzed in BMMC using rat anti-serotonin (upper panel) and rat anti-mouse mMCP-6 (lower panel) using confocal microscopy. Representative single optical sections and overlay (Merge) images are shown. (B) Ultrastructural colocalization analysis of RPMC using VAMP-8 (10 nm GP, black arrows) and mouse anti-serotonin (20 nm GP, white arrows). The inset shows VAMP-8 granule matrix labelling on vesicular-like structures. (C) Colocalization of VAMP-8 with SG marker serotonin was analyzed in unstimulated (NS) and PMA/ionomycin (3 min) stimulated (S) BMMCs. Cells were stained with rabbit anti-VAMP-8 and mouse anti-serotonin. For comparison relative localisation to plasma membrane marker c-kit (rat mAb) is shown. Cells were analyzed by confocal microscopy. Representative single optical sections as well as two (2C) and three color (3C) overlay images are shown. Compartments showing overlap for two colour and three colours appear as yellow and white, respectively. Bars, 5 µm.

Figure 6. **Localisation of syntaxin-3, serotonin and c-kit in resting and stimulated WT and VAMP-8-deficient BMMCs.**

Colocalization of SG marker syntaxin-3 and serotonin was analyzed in non-stimulated (NS) and PMA/ionomycin (3 min) stimulated (S) WT (A) and VAMP-8-deficient (B) BMMCs. Cells were stained with rabbit anti-syntaxin-3 and mouse anti-serotonin. For comparison relative localisation to the plasma membrane marker c-kit (rat mAb) is shown. Cells were analyzed by confocal microscopy. Representative single optical

sections as well as two (2C) and three color (3C) overlay images are shown. Compartments showing overlap for two colour and three colours appear as yellow and white, respectively. Bars, 5 μm.

Figure 7. **Localisation of unprocessed TNF in IL-1β-stimulated WT and VAMP-8-deficient BMMCs.**

(A) VAMP-8-deficient and WT BMMCs were exposed to vehicle (3h). Cells were then stained with anti-TNF and anti-VAMP-8 or anti-VAMP-3 as indicated. (B) VAMP-8-deficient and WT BMMCs were stimulated with 25 ng/ml IL-1β (3 h) in the presence of 50 μM TAPI, which inhibits cleavage of the membrane precursor form of TNF. Cells were stained with anti-TNF and anti-VAMP-8 or anti-VAMP-3 as indicated and were then analyzed by confocal microscopy. Representative single optical sections are shown. In the two-color overlay image (M), compartments containing both markers appear as light blue.

Table I: Quantification of ultrastructural features of VAMP-8 +/+ and -/- BMMC

Mice & Experiments	Granule Size (% small granules)	Number of SG/cell (Mean ± SEM)	Number of immature[a] SG/cell (Mean ± SEM)
VAMP-8 WT Exp 1 (n = 47) Exp 2 (n = 25)	 60 % 65 %	 43.4 ± 3.0 22.3 ± 2.5	 **9.3 ± 1.2**[b] **9.1 ± 2.3**
VAMP-8-deficient Exp 1 (n = 59) Exp 2 (n = 42)	 61 % 59 %	 36.0 ± 3.0 22.6 ± 1.8	 5.8 ± 0.56 5.3 ± 1.00

a) immature granules were defined as electron-lucent granules; mature granules were considered as those filled with electron dense material.

b) statistically significant differences ($p < 0.05$) are indicated in bold

Fig. 1: N. Tiwari et al

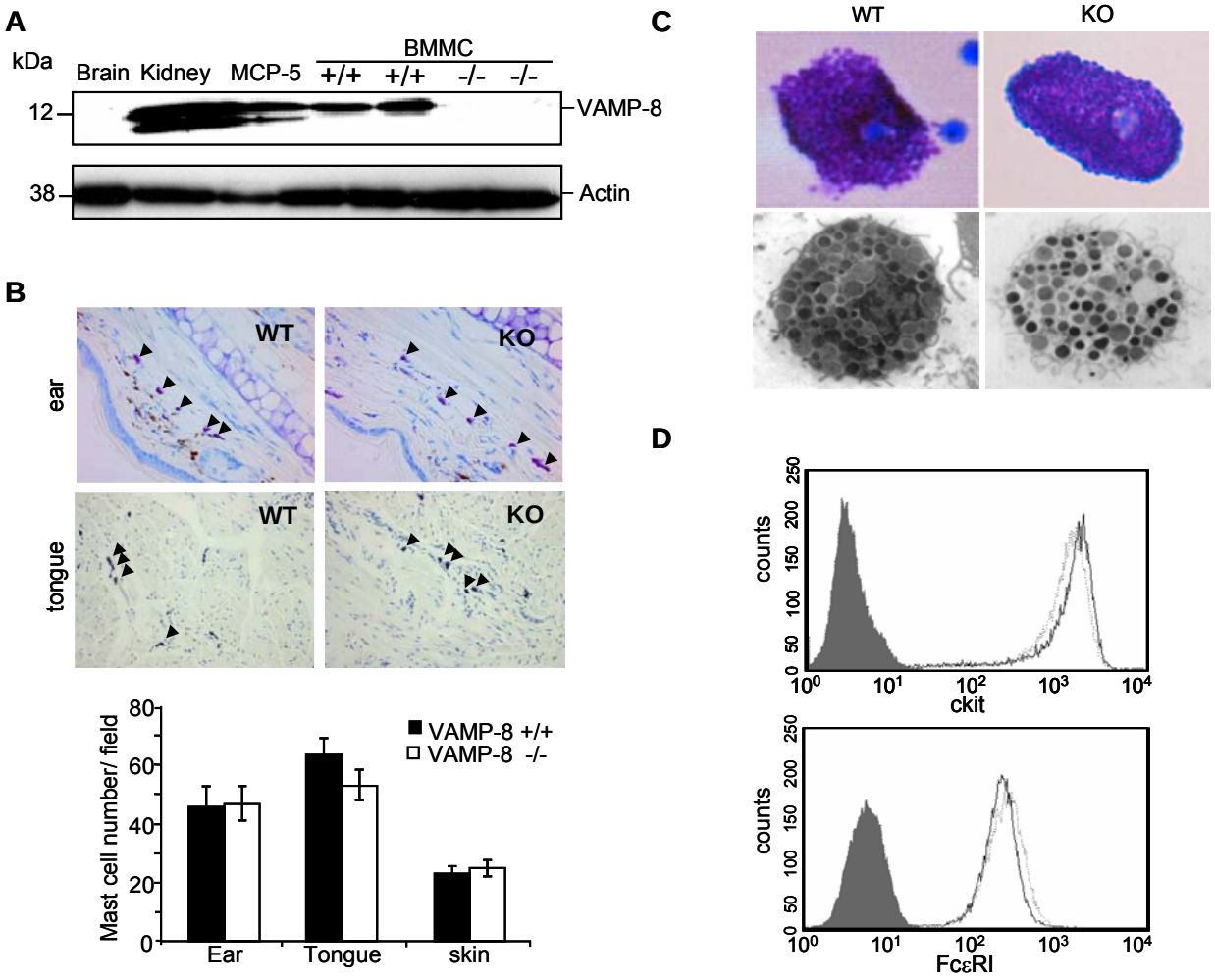

Fig. 2 : N. Tiwari et al

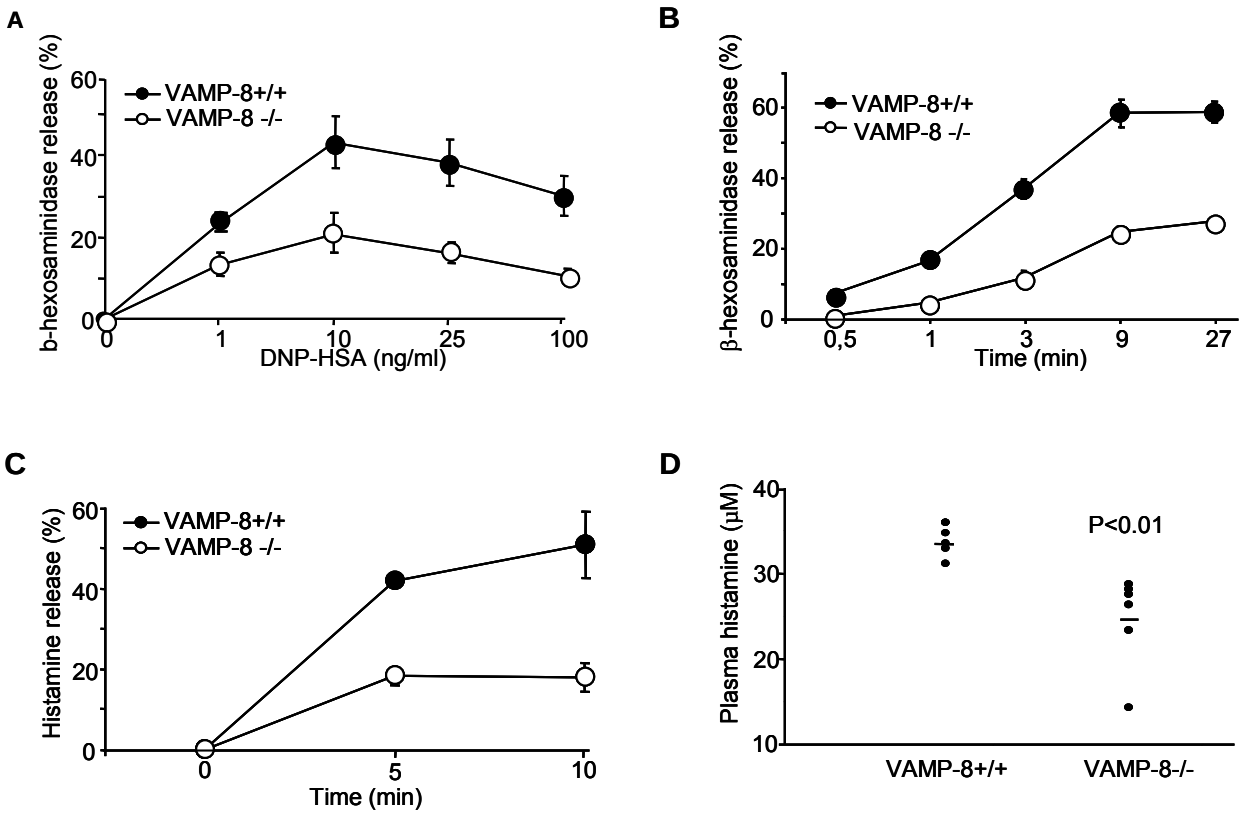

Fig. 3: N. Tiwari et al

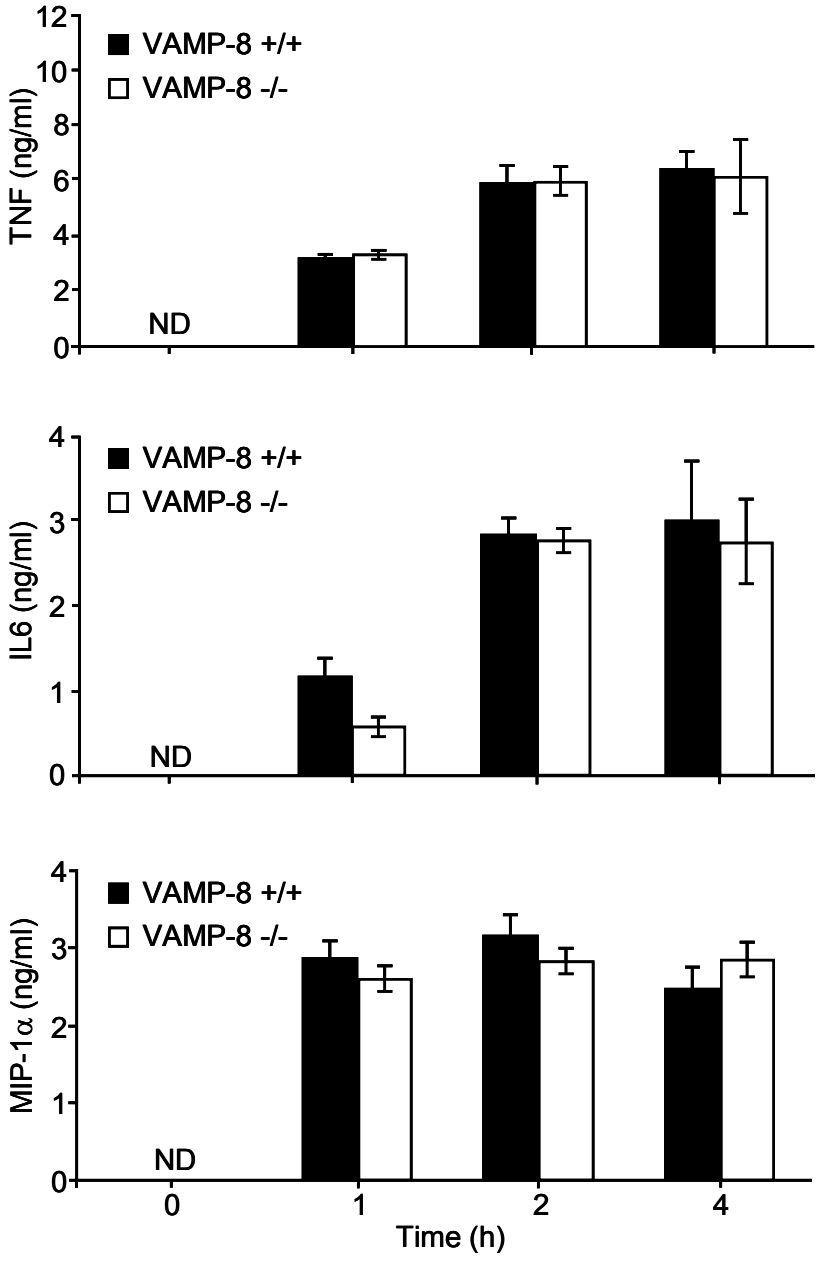

Fig. 4: N. Tiwari et al

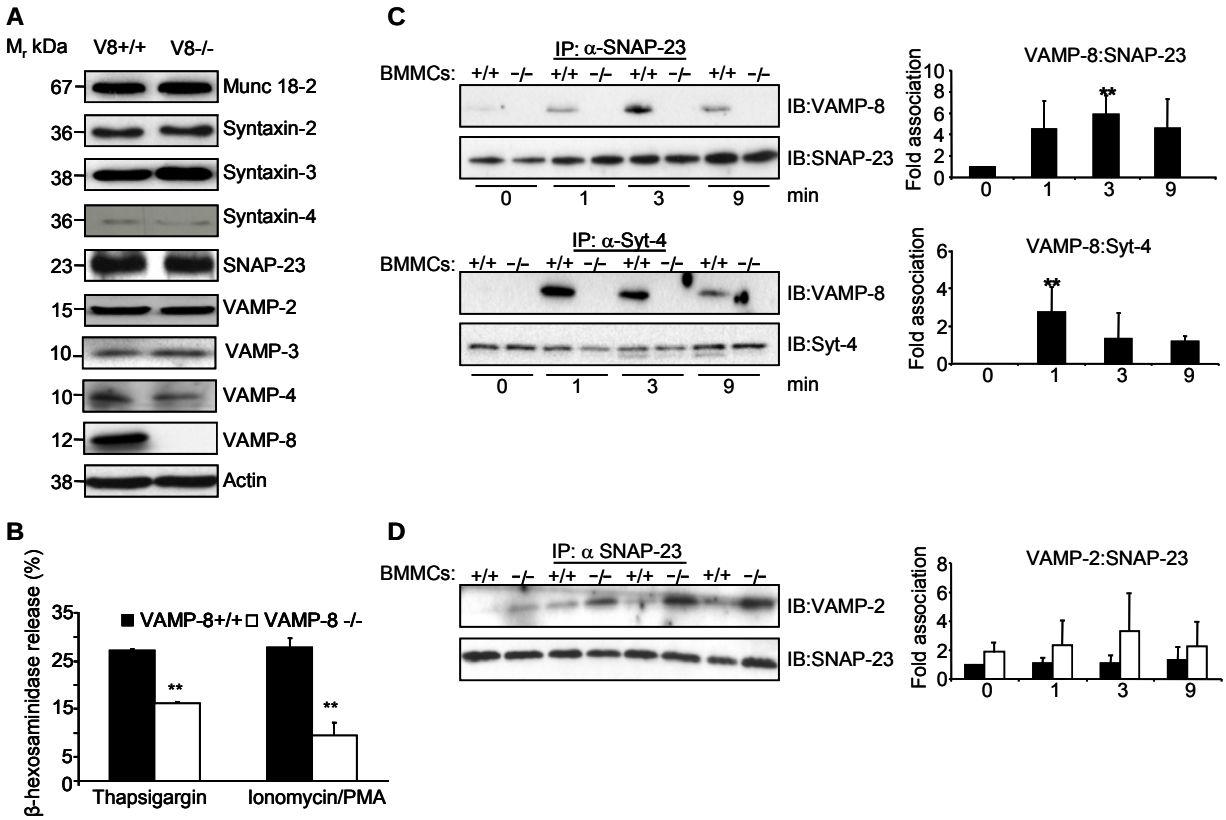

Fig. 5: N. Tiwari et al

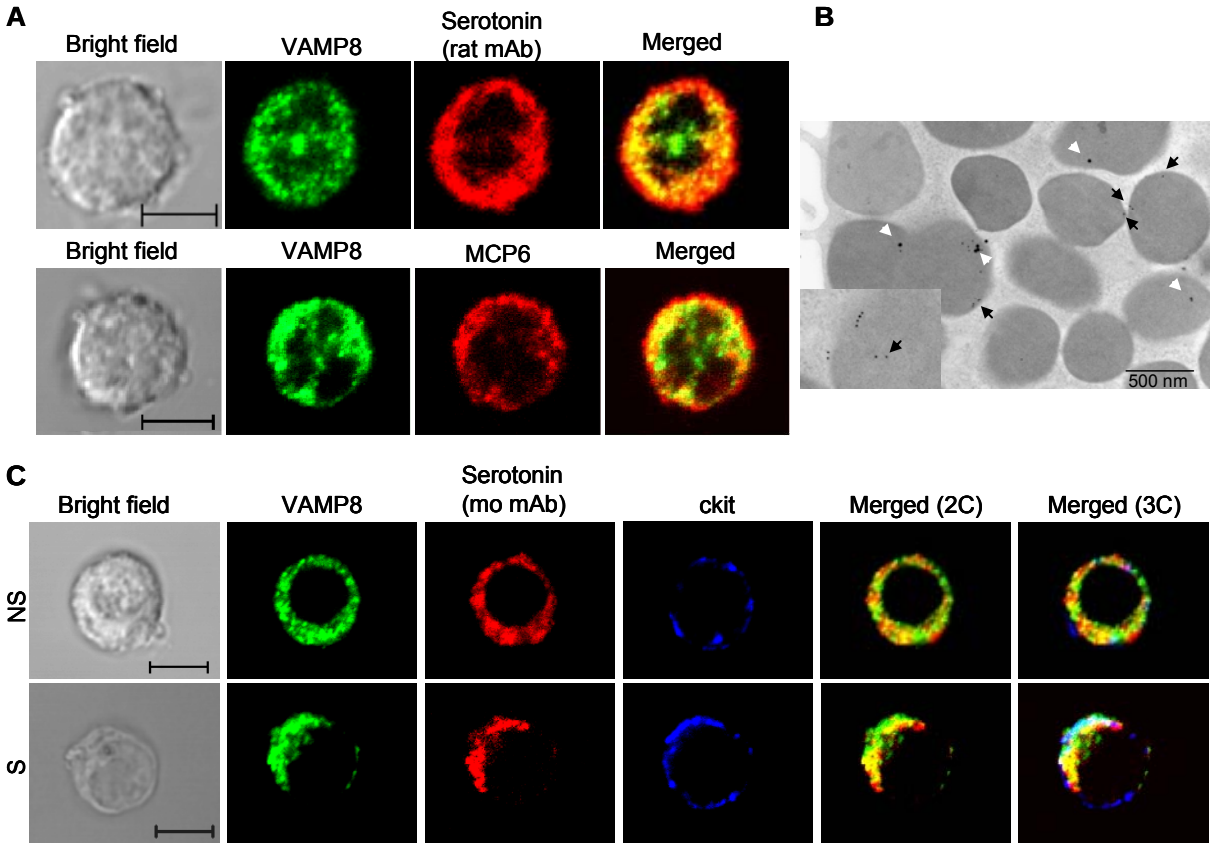

Fig. 6: N. Tiwari et al

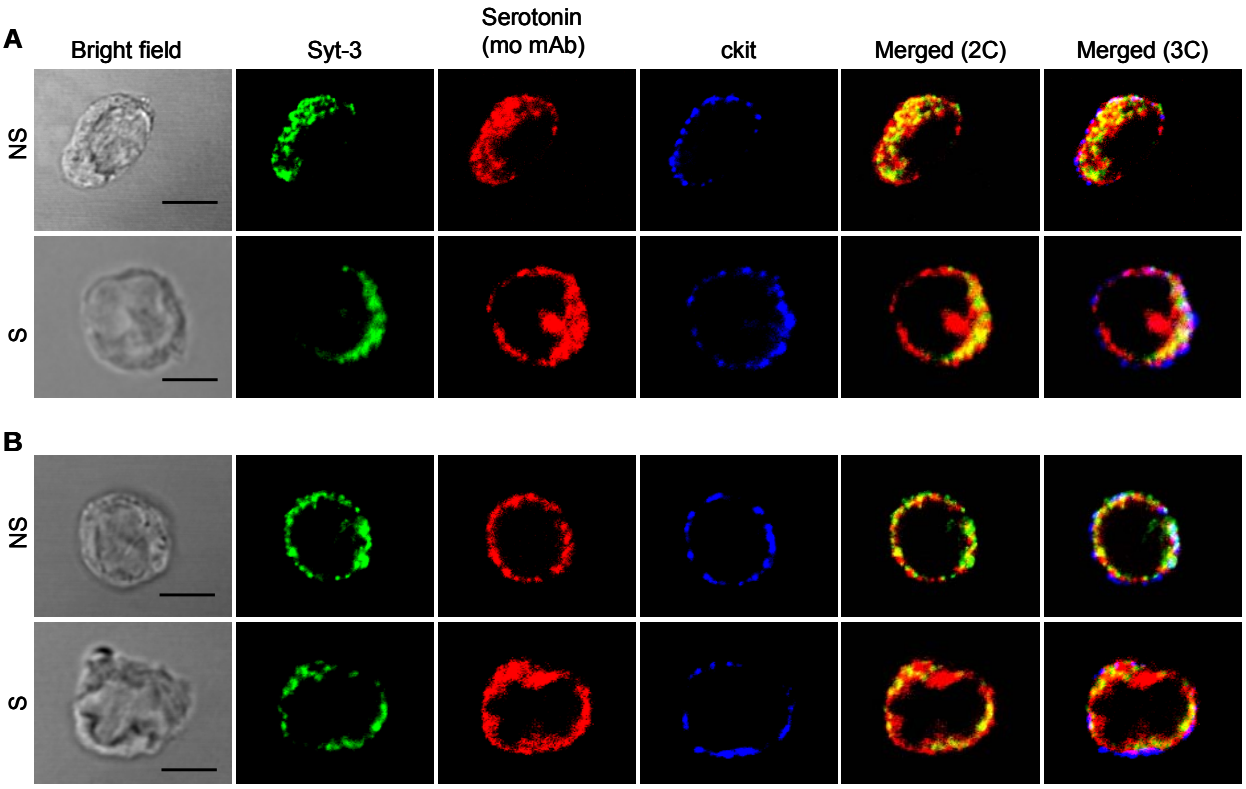

Fig. 7: N. Tiwari et al

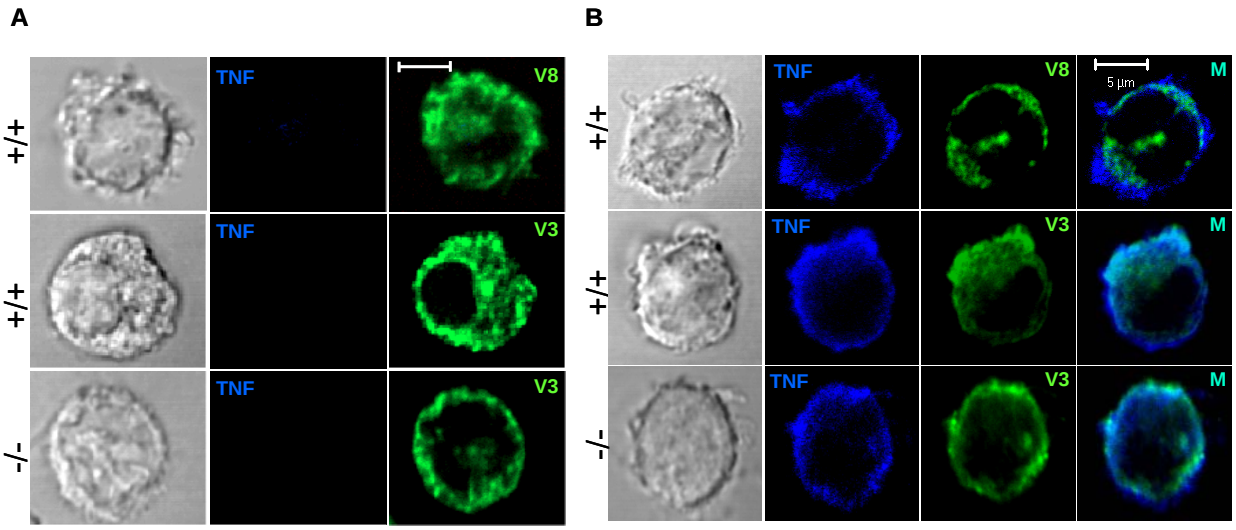

Prepublished online January 18, 2008;
doi:10.1182/blood-2007-07-103309

VAMP-8 segregates mast cell preformed mediator exocytosis from cytokine trafficking pathways

Neeraj Tiwari, Cheng-Chun Wang, Cristiana Brochetta, Gou Ke, Francesca Vita, Zeng Qi, Juan Rivera, Maria Rosa Soranzo, Giuliano Zabucchi, Wanjin Hong and Ulrich Blank

Blood (print ISSN 0006-4971, online ISSN 1528-0020), is published weekly by the American Society of Hematology, 2021 L St, NW, Suite 900, Washington DC 20036.